HHS Public Access

Author manuscript

Biochemistry. Author manuscript; available in PMC 2015 May 25.

Published in final edited form as:

Biochemistry. 2008 August 5; 47(31): 8007–8015. doi:10.1021/bi800857f.

Structural Transitions of the RING1B C-Terminal Region upon Binding the Polycomb cbox Domain†

Renjing Wang, **Udayar Ilangovan**, **Angela K. Robinson**, **Virgil Schirf**, **Patricia M. Schwarz**, **Eileen M. Lafer**, **Borries Demeler**, **Andrew P. Hinck**, and **Chongwoo A. Kim***

Department of Biochemistry, UniVersity of Texas Health Science Center at San Antonio, MSC 7760, 7703 Floyd Curl DriVe, San Antonio, Texas 78229-3900

Abstract

Polycomb group (PcG) proteins are required for maintaining cell identity and stem cell self-renewal. RING1B and Polycomb (Pc) are two components of a multiprotein complex called polycomb repression complex 1 (PRC1) that is essential for establishing and maintaining long-term repressed gene states. Here we characterize the interaction between the C-terminal region of RING1B (C-RING1B) and the Pc cbox domain. The C-RING1B–cbox interaction displays a 1:1 stoichiometry with dissociation constants ranging from 9.2 to 180 nM for the different Pc orthologues. NMR analysis of C-RING1B alone reveals line broadening. However, when it is in complex with the cbox domain, there is a striking change to the NMR spectrum indicative of conformational tightening. This conformational change may arise from the organization of the C-RING1B subdomains. The C-terminal regions of all PcG RING1 proteins are composed of two stretches of conserved sequences separated by a variable linker sequence. While the entire C-RING1B region is required for cbox binding, the N- and C-terminal halves of C-RING1B can be separated and are able to interact, suggesting the presence of an intramolecular interaction within C-RING1B. The flexibility within the C-RING1B structure allowing transitions between the intramolecular bound and unbound states may cause the broadened peaks of the C-RING1B NMR spectrum. Binding the cbox domain stabilizes C-RING1B, whereby broadening is eliminated. The presence of flexible regions could allow C-RING1B to bind a variety of different factors, ultimately recruiting RING1B and its associated PcG proteins to different genomic loci.

Polycomb group (PcG)[1] proteins are gene regulatory proteins that control hundreds of genes that are important for development, stem cell regulation, and cancer (1, 2). They function as multiprotein complexes that act at the level of chromatin, maintaining the repressed state of genes over many cell divisions. PcG proteins are known to silence genes through multiple

†This work was supported by American Heart Association Grant 0830111N (C.A.K.). The UltraScan development is supported by National Institutes of Health Grant RR022200 (B.D.). A.P.H. is supported by the National Institutes of Health (GM49034) and the Robert A. Welch Foundation (AQ1431). Support for the Macromolecular Structure (NMR) and the UTHSCSA Center for Macromolecular Interaction (SPR and AUC) cores from the UTHSCSA ERC and SACI (5P30CA5174) is gratefully acknowledged.

*To whom correspondence should be addressed. chong@biochem.uthscsa.edu. Phone: (210) 567-8779. Fax: (210) 567-8778.

[1]Abbreviations: PcG, polycomb group; PRC1, polycomb repression complex 1; PRC2, polycomb repression complex 2; C-RING1B, conserved C-terminal region of RING1B; K_d, equilibrium dissociation constant; E(z), Enhancer of *zeste*; Esc, extra sex combs; Su(z)12, suppressor of *zeste* 12; Ph, polyhomeotic; Psc, posterior sex combs; Pc, polycomb; MBP, maltose binding protein; SPR, surface plasmon resonance; NMR, nuclear magnetic resonance.

mechanisms, including the post-translational modification of histones (methylation and ubiquitination) and the creation of repressive higher-order chromatin structures.

Each PcG protein functions within the context of a multiprotein complex. For example, polycomb repression complex 2 (PRC2) is a multiprotein complex which possesses methyltransferase activity (3–6). PRC2 core members include the enhancer of *zeste* [E(z)], extra sex combs [Esc; embryonic ectoderm development (EED) is the mammalian orthologue], the suppressor of *zeste* 12 [Su(z)12], and P55. While the SET domain within E(z) is responsible for catalyzing the methyl transfer, this activity is dependent on the presence of the other components of PRC2. The core members of a different PcG complex called polycomb repression complex 1 (PRC1) are polyhomeotic (Ph), posterior sex combs (Psc) (Bmi-1 and Mel-18 are two mammalian orthologues), RING1 (RING1A and RING1B in mammals), and polycomb (Pc) (7, 8). PRC1 has the ability to compact chromatin (9) and inhibit the action of chromatin remodeling enzymes (10). In addition, the RING finger domains found in the RING1 proteins and Bmi-1 (and Mel-18) associate to form a heterodimer which acts as a ubiquitin ligase for the ubiquitination of histone H2A lysine 119 (11, 12). PRC1 has also been observed to be associated with proteins involved in promoting transcription such as TBP, TFIIF, and TFIIB (13, 14), perhaps indicative of an alternative mode of repression that targets the general transcriptional machinery.

Pc, the original member of the PcG, contains two conserved domains: the N-terminal chromo domain and an ~40-amino acid region at the C-terminus termed the cbox domain (Figure 1). The *Drosophila* Pc chromo domain is primarily targeted to trimethylated lysine 27 of histone 3 (H3K27me3) (15, 16), but a recent study has shown that among the mammalian Pc orthologues, the binding preferences for different methylated lysines on H3 can vary (17). The C-terminal cbox domain, like the chromo domain, is required for proper *Drosophila* development (18). Yeast twohybrid studies have shown that the cbox domain is sufficient for binding to the PcG RING1 proteins (19, 20). *Drosophila* RING1 and its two mammalian orthologues, RING1A and RING1B, have two conserved regions: an N-terminal RING finger domain that functions as a ubiquitin ligase and a conserved C-terminal region (C-RING1). C-RING1 binds the Pc cbox domain and is composed of two conserved stretches of 50–60 amino acids separated by a variable linker sequence (Figure 1). The interaction between C-RING1 and Pc cbox may represent a means of recruiting the repressive functions of the RING finger heterodimer ubiquitin ligase activity to chromatin.

In this study, we analyzed the interaction between the Pc cbox domain and human C-RING1B. We show that C-RING1B binds the cbox domain in a 1:1 stoichiometry with high affinity for all five human Pc orthologues: cbx2 Pc1 or M33 in mice), cbx4 (Pc2), cbx6, cbx7, and cbx8 (Pc3). We also show that C-RING1B in the absence of the cbox domain possesses some internal flexibility stemming from the linker sequence that separates the two subdomains within C-RING1B. The subdomains can interact in trans, suggesting that within the context of the entire C-RING1B region, they are likely to interact in an intramolecular fashion. Upon binding the Pc cbox domain, a single C-RING1B conformation is stabilized. The interaction between C-RING1B and the Pc cbox domain also induces Pc cbox structure, which is mostly disordered in the absence of C-RING1B. The use of intrinsically disordered regions for protein–protein interactions can expand the repertoire of binding partners by

creating a discrete interaction surface for different binding partners which a nonflexible protein is unable to do. Protein “hubs” are proteins that have not just several but many binding partners (21) and frequently use unstructured protein regions in binding reactions (22, 23). C-RING1B may function in a similar manner to bind the Pc cbox domain and other proteins. These associations would allow RING1B and the repressive activity of PcG proteins associated with RING1B also to be targeted to different genomic sites that are targeted by RING1B’s binding partner.

EXPERIMENTAL PROCEDURES

Protein Preparation

C-RING1B (residues 222–336) and the cbox domains from cbx6, cbx7, and cbx8 were cloned into a modified pET-3c vector which incorporates a MEKTR leader sequence and a C-terminal SRHHHHHH tag to facilitate purification. A C-RING1B clone with the same leader sequence but an alternative C-terminal SRD sequence was cloned into pET-30a for coexpression with the cbx7 cbox domain. The hexahistidine tag on the cbx7 cbox domain was utilized for purification of the C-RING1B–cbx7 cbox domain complex. The C_N- and C_C-RING1B residues used for the two bacterial hybrids are residues 222–274 and 284–336, respectively. The amino acid residues used for all the cbox subcloning into the above-mentioned pET vectors, pBADM-41 + (EMBL) for expression as a fusion with maltose binding protein (MBP) and the two bacterial hybrid vectors pBT and pTRG, are shown in Figure 1C.

All pET vector constructs were expressed in BL21- Gold(DE3) cells (Stratagene) pretransformed with pRARE (Novagen). The C-RING1B–cbox domain complexes were isolated via cotransformation of both the C-RING1B and cbox constructs and then maintenance of the bacterial cells in the presence of both kanamycin and ampicillin along with chloramphenicol to maintain the pRARE plasmid. The pBADM-41 + constructs were expressed in ARI814 cells (24) and induced with 0.2% arabinose. A typical purification of proteins involved resuspending cells from a 1 L culture in 10 mL of 50 mM Tris (pH 8.0), 200 mM NaCl, 25 mM imidazole (pH 7.5), and 1 mM PMSF. The cells were lysed by sonication and all proteins extracted from the soluble lysate using Ni affinity chromatography followed by ion exchange chromatography. All proteins were purified to greater than 99% purity according to their SDS–PAGE analysis.

Native Gel Electrophoresis

The native gel electrophoresis experiments were performed with C-RING1B and the cbox domain from cbx6. We mixed varying molar ratios of both components as indicated in Figure 2A. The binding reaction mixtures were allowed to equilibrate over 30 min at room temperature in 10 mM Tris-HCl (pH 7.8), 50 mM NaCl, and 5 mM β-mercaptoethanol prior to separation of the different species on a 12% native polyacrylamide gel.

Surface Plasmon Resonance

All surface plasmon resonance (SPR) data were collected at room temperature using a Biacore 3000 instrument and analyzed using BIAevaluation 3.0. Solution competition SPR

was used to measure the apparent equilibrium dissociation constants (K_d) for the binding reactions between C-RING1B and all the cbox domains. By this method, the interactants are allowed to come to equilibrium in solution, and then the surface is used to separate bound from free (25). C-RING1B was immobilized on a Biacore Pioneer research-grade CM5 sensor chip at a density of approximately 1500 response units (RU) using amine coupling chemistry (Biacore Inc. amine coupling kit). First, a titration was performed in which varying concentrations of MBP–cbox fusion proteins were introduced into the mobile phase at a rate of 5 μL/min in 10 mM HEPES (pH 7.4), 150 mM NaCl, 3 mM EDTA, 1 mM DTT, and 0.005% Surfactant P20 running buffer to determine the best MBP–cbox protein concentration to be used in the competition experiment. The MBP–cbox protein concentration within the linear range of this initial titration was used in the competition experiments to determine the K_d. For the competition experiments, a series of binding reactions were first set up with the same amount of MBP–cbox protein, determined from the previous titration, mixed with varying amounts of C-RING1B. The reaction mixtures were incubated at room temperature for 2 h to allow equilibrium to be reached before introduction of the solutions over cross-linked C-RING1B. The competition titrations and binding curves are shown in Figure 2B. The plots were fit to a hyperbolic function (Origin 7), and the apparent equilibrium dissociation constants (K_d) were determined from the concentration of C-RING1B at 50% inhibition.

Bacterial Two-Hybrid Assay

Chemical competent Bacteriomatch reporter cells (Stratagene) were transformed with miniprepped DNA and plated out onto LB agar plates with 100 μg/mL ampicillin, 50 μg/mL tetracycline, and 25 μg/ mL chloramphenicol. Plates were observed for colonies after the plates had been incubated for 16 h at 37 °C.

NMR Spectroscopy

NMR samples for both C-RING1B alone and the C-RING1B–cbx7 cbox complex were prepared in M9 minimal medium containing 0.1% $^{15}NH_4Cl$. The samples were prepared to a concentration of 1 mM for panels A and B of Figure 4, 100 μM for panels C and D of Figure 4, and 300 μM for panel E of Figure 4. All samples were prepared in 10 mM $NaPO_4$ buffer (pH 6.0), 50 mM NaCl, and 5% D_2O. All spectra were recorded on a Bruker Av700 spectrometer equipped with an actively shielded z-gradient triple-resonance probe at 310 K. Spectra were processed with NMRPipe (26).

Analytical Ultracentrifugation

All sedimentation experiments were performed with a Beckman Optima XL-I instrument at the Center for Analytical Ultracentrifugation of Macromolecular Assemblies (CAUMA) at the University of Texas Health Science Center at San Antonio. Sedimentation equilibrium data were analyzed with UltraScan, version 9.4 (27). Hydrodynamic corrections for buffer conditions were made according to data published by Laue et al. (28), and as implemented in UltraScan. The partial specific volumes of C-RING1B and cbx7 were estimated from peptide sequence according to the method of Durchschlag (29), and as implemented in UltraScan, and were found to be 0.7279 and 0.7127 cm^3/g, respectively, and 0.7248 cm^3/g

for the 1:1 complex. Rayleigh interference scans were collected at equilibrium at four speeds (28.4K, 34.0K, 38.7K, and 43.0K rpm). Data from all speeds were fitted globally with the fixed molecular mass distribution method (27) by using 50 molecular mass slots ranging between 1 and 50 kDa. The loading concentration for these experiments was approximately 450 μM for both C-RING1B alone and C-RING1B in complex with the cbx7 cbox domain. All samples were spun in two-channel Epon-filled centerpieces (Beckman Coulter) in an AN-60-TI rotor.

RESULTS

C-RING1B Binds the cbox Domain in a 1:1 Molar Ratio with High Affinity

In our analysis of the C-RING1B–cbox interactions, we wished to first establish the stoichiometry between C-RING1B and the cbox domain. We used native gel electrophoresis with varying ratios of C-RING1B and the cbox domain from cbx6 (Figure 2A). A 1:1 molar ratio of the two components results in a single band that migrates slower than the cbx6 cbox domain and faster than C-RING1B. Experiments performed with a molar excess of either the cbx6 cbox domain or C-RING1B resulted in the appearance of the band corresponding to that of the excess component alone. This result suggests C-RING1B and the cbx6 cbox domain form a stable complex with a 1:1 molar ratio. Additional data in support of this stoichiometry were obtained from analytical ultracentrifugation experiments described below.

We next sought to measure the strength of the interactions. For this purpose, we used solution competition surface plasmon resonance (SPR) to determine the equilibrium dissociation constant (K_d). In these experiments, we incubated varying concentrations of C-RING1B with a fixed concentration of a maltose binding protein-fused cbox domain and allowed the reactions to come to equilibrium in solution. We then injected these reaction mixtures over a surface with immobilized C-RING1B to separate bound MBP–cbox complex from free. The concentration of C-RING1B in solution required to inhibit half of the binding to immobilized C-RING1B is equivalent to the K_d (25). While MBP alone did not bind to the immobilized C-RING1B surface, all the cbox domain MBP fusion proteins exhibited strong interaction with immobilized C-RING1B which was inhibited by introduction of varying amounts of C-RING1B in the mobile phase. Figure 2B shows the competition titration experiments for the C-RING1B–cbox domain interactions along with the plots of the percent inhibition versus the C-RING1B concentration in solution. The plots are fit to a hyperbolic function, and K_d values are determined from the concentration of C-RING1B at 50% inhibition. The K_d values for the interaction between C-RING1B and the various cbox domains range from a very stable 9.2 nM for cbx7 to 180 nM for cbx8 and cbx6. Interestingly, the *Drosophila* Pc cbox domain also shows a very strong interaction (K_d) 38 nM) indicative of the conserved binding function between the *Drosophila* and human proteins. This conserved function over evolution is perhaps not surprising as ectopic expression of the closely related human RING1A is able to rescue a *Drosophila* phenotype associated with missing the *Drosophila* RING1 protein (30).

C-RING1B Is Composed of Two Interacting Subdomains

The C-RING1 region of the PcG RING1 proteins contains two conserved blocks of sequences separated by a variable-length linker sequence (Figure 1B). We sought to determine the role of each of the subdomains in the binding reaction with the cbox domain. To carry out biochemical characterization of each subdomain, we first attempted to isolate the individual subdomains, C_N-RING1B and C_C-RING1B for the N- and C-terminal halves of C-RING1B, respectively. While the entire C-RING1B can be expressed in soluble form in bacteria and prepared at high concentrations, neither of the two C-RING1B subdomains could be isolated for biochemical analysis. We turned to a bacterial two-hybrid assay to assess which of the two subdomains is responsible for binding the cbox domain. The bacterial two-hybrid assay offers an advantage in that even a small percentage of active proteins within the bacterial cell can lead to expression of the reporter gene. We fused C_N- and C_C-RING1B and the cbx7 cbox domain to both the λ cI DNA binding protein and the N-terminal transactivation domain of *Escherichiacoli* RNA polyermase (RNAP) and carried out bacterial twohybrid experiments testing for interaction between all combinations of the three proteins, including their ability to self-associate (Figure 3A). Neither C_N-RING1B nor C_C-RING1B alone is able to interact with the cbx7 cbox domain as indicated by the inability of each to express the β-lactamase reporter gene and survive on the ampicillin agar medium. The interaction between the entire C-RING1B and the cbx7 cbox domain is strong (K_d) 9.2 nM) and can easily be detected using the bacterial two-hybrid assay (Figure 3B), and thus, the negative results for the interaction between the C-RING1B subdomains and the cbx7 cbox domain appear not to be due to assay limitations but rather the inability of either C_N-RING1B or C_C-RING1B to bind cbox on its own. Surprisingly, we observed bacterial growth that tests the association between C_N-RING1B and C_C-RING1B. These results show that C-RING1B is composed of two domains which can interact in trans, and both of these domains are required to bind cbox.

The cbox Domain Stabilizes C-RING1B

Given that the two subdomains of C-RING1B are required to bind the cbox domain, we sought to monitor any structural changes that may occur in binding the cbox domain. We monitored the structure of C-RING1B using NMR spectroscopy. We isolated isotopically labeled C-RING1B as well as the entire C-RING1B–cbx7 cbox complex with ^{15}N. The complex was obtained from bacterial cells coexpressing both proteins and purified utilizing a hexahistidine tag present only on the cbox domain. We chose the cbx7 cbox domain because it demonstrated the greatest affinity for the C-RING1B domain in the SPR experiments described above. The two-dimensional ^{1}H–^{15}N HSQC spectrum of C-RING1B alone displays a disperse pattern of cross-peaks indicative of a structured protein but exhibits fewer resonances [84 of 118 possible (Figure 4A)] than expected. The C-RING1B–cbx7 cbox domain complex shows considerable differences in the HSQC spectrum (Figure 4B). The chemical shifts of the spectrum of the C-RING1B–cbx7 cbox domain complex are even more dispersed than those of C-RING1B alone. Furthermore, there is a striking increase in the number of observed resonances. We observe 167 of a possible 170 backbone amide signals for the C-RING1B–cbx7 cbox domain complex. Thus, resonances not observed in the spectrum of C-RING1B alone appear in the presence of the cbx7 cbox domain. To

confirm that the chemical shift dispersion occurs within C-RING1B, we recorded the HSQC spectrum on a sample of ^{15}N-labeled C-RING1B alone (Figure 4C) and then re-recorded an HSQC spectrum after adding an equimolar amount of unlabeled cbx8 domain to the same C-RING1B sample (Figure 4D). Even with the weaker affinity for C-RING1B, the cbx8 cbox domain also causes dispersion of the chemical shifts which was observed with cbx7. As only C-RING1B is labeled with ^{15}N, the dispersion seen in Figure 4D can be attributed to only C-RING1B.

The C-RING1B–cbox interaction also has a stabilizing affect on the cbox domain. The one-dimensional ^{1}H NMR spectra of the cbox domains from both cbx6 and cbx8 show little to no evidence of tertiary structure as indicated by the lack of signals that are shifted either downfield or upfield relative to the random coil limits for backbone amides or side chain methyls, respectively (Figure 4E). Due to the lack of solubility, we were unable to obtain NMR samples for any of the other cbox domains. As noted above, the ^{1}H–^{15}N HSQC spectrum of the co-expressed, copurified C-RING1B–cbx7 cbox domain complex is well-dispersed, indicative of a very well-ordered complex. Thus, it would seem likely that the cbox domain exists in a single structured conformation only when associated with the C-RING1B domain.

C-RING1B Dimerization Inhibited by Interaction with the cbox Domain

A recent report demonstrated the ability of C-RING1B to dimerize with an equilibrium dissociation constant (K_d) of approximately 200 μM (31). Yeast two-hybrid results have also shown that C-RING1A can self-associate (32). Given the effect of cbox on C-RING1B as observed in their ^{1}H–^{15}N HSQC spectra, we wondered how cbox binding to C-RING1B influences its oligomerization. We analyzed both C-RING1B alone and in complex with the cbx7 cbox domain using analytical ultracentrifugation (Figure 5). Over an approximate concentration range from 0 to 500 μM in the sedimenting sample, C-RING1B alone shows a molecular mass distribution between 16000 and 24000 Da (Figure 5A), indicative of a monomer–dimer equilibrium for 14 kDa C-RING1B and consistent with reports of C-RING1B homodimerization (31). In contrast, the C-RING1B–cbx7 cbox domain complex over an equivalent concentration range shows a molecular mass distribution from 16000 to 19000 Da, indicative of a 1:1 heterodimer complex (Figure 5B). Importantly, not only is the molecular mass distribution considerably narrower than that of C-RING1B alone, but it also does not exceed 19000 Da for the complex. These results clearly indicate C-RING1B–cbx7 cbox domain interaction precludes C-RING1B homodimerization and the stoichiometry is 1:1, consistent with the stoichiometry determined from the native gel analysis.

DISCUSSION

We have biochemically characterized the interaction between C-RING1B and the cbox domain. The stoichiometry of the C-RING1B–cbox domain interaction is 1:1 with dissociation constants ranging from 9.2 to 180 nM for all Pc orthologue cbox domains. C-RING1B exists as two separate subdomains that are able to interact, and both of these are required for the interaction with the cbox domain. There are three structural consequences of the C-RING1B–cbox domain interaction. First, C-RING1B undergoes a transition from a

nonrigid, flexible structure to a more rigid state upon binding the cbox domain. Second, the nonstructured cbox peptide also undergoes a transition from a random coil to an ordered state. Third, homodimerization of C-RING1B is inhibited by the interaction with the cbx7 cbox domain.

C-RING1B Organization

Our analysis of C-RING1B alone revealed only 84 of a possible 118 backbone N–H correlations in its $^{1}H–^{15}N$ HSQC NMR spectrum. The absence of some signals is consistent with previously reported observations for C-RING1B whose TOCSY and NOESY spectra exhibited peak broadening (31). One possible cause of the missing peaks is rapid exchange between the backbone amide hydrogens and solvent. This appears unlikely because the spectrum of the C-RING1B–cbx7 cbox domain complex is entirely different, showing nearly all possible peaks despite the NMR sample being under conditions identical to those of C-RING1B alone. An alternative reason for the missing peaks could be conformational exchange broadening. There are two possible causes for C-RING1B conformational exchange broadening. One possibility is the monomer–dimer equilibrium of C-RING1B. However, due to the unusually large proportion of the C-RING1B residues with broadened peaks, it does not seem likely that dimerization alone would account for the broadening. An alternative source of conformational exchange broadening is the intramolecular interaction within C-RING1B made possible by the flexible linker that separates the two subdomains within C-RING1B.

The sequence alignment of the PcG RING1 proteins (Figure 1B) shows two subdomains separated by a variable length linker sequence. Both subdomains are unstable when expressed individually and cannot be isolated in a soluble form. Using a bacterial two-hybrid assay, we observe that while neither of the two subdomains, C_N-RING1B and C_CRING1B, is able to bind the cbox domain, C_N-RING1B can associate with C_C-RING1B in trans (Figure 3A). These results suggest that rather than being a single domain where the variable length linker sequence is a loop within the structure, C-RING1B possesses intrinsic flexibility and is composed of two separate halves that are able to independently fold or be induced to fold upon their interaction. If this intramolecular interaction lacks sufficient binding energy to maintain a fully defined structure and freely undergoes transitions between its “open” and “closed” states, NMR peak broadening would occur.

The interaction between C-RING1B and the cbox domains results in a considerable conformational change to both proteins. In addition to the intrinsic flexibility of C-RING1B described above, the one-dimensional NMR spectra of the cbox domains show little or no evidence of tertiary structure. However, when C-RING1B binds the cbox domain, a conformational “tightening” occurs in which both proteins are now very much ordered as indicated by the dispersed nature and the appearance of nearly all possible $^{1}H–^{15}N$ correlation peaks in the HSQC spectrum of the complex compared to those of the individual components. Furthermore, dimerization of C-RING1B is precluded by cbox binding.

C-RING1B Binds Other Proteins

The intrinsic flexibility within both C-RING1B and its binding partners could enable C-RING1B to interact with numerous targets, as observed for “hub” proteins (22, 23). Hubs frequently utilize unstructured regions in binding reactions to facilitate binding diversity. One category of hubs involves the use of a flexible linker between functional domains, not unlike the two subdomains of C-RING1B. The ability to associate with numerous binding partners may enable the PcG RING1 proteins to be targeted to a variety of genomic loci depending on the identity of its binding partner. For example, when associated with the Pc cbox domain, RING1B, along with Bmi-1 and Ph, can be recruited to modified chromatin by the recognition of the Pc chromo domain for methylated histones. Other C-RING1B binding partners that have been identified include the E2F-associated factors YAF2 and RYBP and methylated DNA binding protein MBD1 (33–35). Additionally, a recent proteomic study identified 20 new proteins that associate with RING1B (36). Whether these new binding partners directly interact with C-RING1B is not known but remains a possibility. While the Pc cbox domains are highly conserved in their sequence (Figure 1C), the other proteins that associate with C-RING1B exhibit little sequence similarity with the cbox domains. Despite this lack of sequence conservation, it remains possible that proteins like YAF2 and RYBP bind to C-RING1B in a fashion similar to those of the cbox domains and stabilize the C-RING1B disorder. The intrinsic flexibility of C-RING1B and its binding partner may provide new protein–protein contacts that are different from the ones utilized in theC-RING1B–cbox interactions but still leads to overall stabilization of the complex like the cbox domains. The consequence of having a diverse array of binding partners would allow the PcG RING1 proteins to be recruited to different locations in the genome.

Summary

We have characterized a binding reaction that is important for the assembly of PRC1. C-RING1B binds to the cbox domains of all Pc orthologues with high affinity. In the absence of the cbox domain, C-RING1B contains two subregions that are able to interact. When C-RING1B binds the Pc cbox domain, its conformation is stabilized into a single ordered state. Rather than using a lock-and-key mode of binding, the use of a binding mechanism that resembles the induced fit interaction may allow C-RING1B to have more binding partners. The consequences of having multiple binding partners would allow the PcG RING1 proteins to be recruited to different locations in the genome.

ACKNOWLEDGMENT

We thank Dr. P. John Hart for helpful comments on the manuscript. pBADM-41 + was provided by EMBL.

REFERENCES

1. Sparmann A, van Lohuizen M. Polycomb Silencers Control Cell Fate, Development and Cancer. Nat. Rev. Cancer. 2006; 6:846–856. [PubMed: 17060944]
2. Schwartz YB, Pirrotta V. Polycomb Silencing Mechanisms and the Management of Genomic Programmes. Nat. Rev. Genet. 2007; 8:9–22. [PubMed: 17173055]
3. Czermin B, Melfi R, McCabe D, Seitz V, Imhof A, Pirrotta V. *Drosophila* Enhancer of Zeste/ESC Complexes have a Histone H3 Methyltransferase Activity that Marks Chromosomal Polycomb Sites. Cell. 2002; 111:185–196. [PubMed: 12408863]

4. Muller J, Hart CM, Francis NJ, Vargas ML, Sengupta A, Wild B, Miller EL, O'Connor MB, Kingston RE, Simon JA. Histone Methyltransferase Activity of a *Drosophila* Polycomb Group Repressor Complex. Cell. 2002; 111:197–208. [PubMed: 12408864]
5. Kuzmichev A, Nishioka K, Erdjument-Bromage H, Tempst P, Reinberg D. Histone Methyltransferase Activity Associated with a Human Multiprotein Complex Containing the Enhancer of Zeste Protein. Genes Dev. 2002; 16:2893–2905. [PubMed: 12435631]
6. Cao R, Wang L, Wang H, Xia L, Erdjument-Bromage H, Tempst P, Jones RS, Zhang Y. Role of Histone H3 Lysine 27 Methylation in Polycomb-Group Silencing. Science. 2002; 298:1039–1043. [PubMed: 12351676]
7. Shao Z, Raible F, Mollaaghababa R, Guyon JR, Wu CT, Bender W, Kingston RE. Stabilization of Chromatin Structure by PRC1, a Polycomb Complex. Cell. 1999; 98:37–46. [PubMed: 10412979]
8. Francis NJ, Saurin AJ, Shao Z, Kingston RE. Reconstitution of a Functional Core Polycomb Repressive Complex. Mol. Cell. 2001; 8:545–556. [PubMed: 11583617]
9. Francis NJ, Kingston RE, Woodcock CL. Chromatin Compaction by a Polycomb Group Protein Complex. Science. 2004; 306:1574–1577. [PubMed: 15567868]
10. Francis NJ, Kingston RE. Mechanisms of Transcriptional Memory. Nat. Rev. Mol. Cell Biol. 2001; 2:409–421. [PubMed: 11389465]
11. Wang H, Wang L, Erdjument-Bromage H, Vidal M, Tempst P, Jones RS, Zhang Y. Role of Histone H2A Ubiquitination in Polycomb Silencing. Nature. 2004; 431:873–878. [PubMed: 15386022]
12. de Napoles M, Mermoud JE, Wakao R, Tang YA, Endoh M, Appanah R, Nesterova TB, Silva J, Otte AP, Vidal M, Koseki H, Brockdorff N. Polycomb Group Proteins Ring1A/B Link Ubiquitylation of Histone H2A to Heritable Gene Silencing and X Inactivation. Dev. Cell. 2004; 7:663–676. [PubMed: 15525528]
13. Breiling A, Turner BM, Bianchi ME, Orlando V. General Transcription Factors Bind Promoters Repressed by Polycomb Group Proteins. Nature. 2001; 412:651–655. [PubMed: 11493924]
14. Saurin AJ, Shao Z, Erdjument-Bromage H, Tempst P, Kingston RE. A *Drosophila* Polycomb Group Complex Includes Zeste and dTAFII Proteins. Nature. 2001; 412:655–660. [PubMed: 11493925]
15. Fischle W, Wang Y, Jacobs SA, Kim Y, Allis CD, Khorasanizadeh S. Molecular Basis for the Discrimination of Repressive Methyl-Lysine Marks in Histone H3 by Polycomb and HP1 Chromodomains. Genes Dev. 2003; 17:1870–1881. [PubMed: 12897054]
16. Min J, Zhang Y, Xu RM. Structural Basis for Specific Binding of Polycomb Chromodomain to Histone H3 Methylated at Lys 27. Genes Dev. 2003; 17:1823–1828. [PubMed: 12897052]
17. Bernstein E, Duncan EM, Masui O, Gil J, Heard E, Allis CD. Mouse Polycomb Proteins Bind Differentially to Methylated Histone H3 and RNA and are Enriched in Facultative Heterochromatin. Mol. Cell. Biol. 2006; 26:2560–2569. [PubMed: 16537902]
18. Franke A, Messmer S, Paro R. Mapping Functional Domains of the Polycomb Protein of *Drosophila melanogaster*. Chromosome Res. 1995; 3:351–360. [PubMed: 7551550]
19. Satijn DP, Gunster MJ, van der Vlag J, Hamer KM, Schul W, Alkema MJ, Saurin AJ, Freemont PS, van Driel R, Otte AP. RING1 is Associated with the Polycomb Group Protein Complex and Acts as a Transcriptional Repressor. Mol. Cell. Biol. 1997; 17:4105–4113. [PubMed: 9199346]
20. Schoorlemmer J, Marcos-Gutierrez C, Were F, Martinez R, Garcia E, Satijn DP, Otte AP, Vidal M. Ring1A is a Transcriptional Repressor that Interacts with the Polycomb-M33 Protein and is Expressed at Rhombomere Boundaries in the Mouse Hindbrain. EMBO J. 1997; 16:5930–5942. [PubMed: 9312051]
21. Han JD, Bertin N, Hao T, Goldberg DS, Berriz GF, Zhang LV, Dupuy D, Walhout AJ, Cusick ME, Roth FP, Vidal M. Evidence for Dynamically Organized Modularity in the Yeast Protein-Protein Interaction Network. Nature. 2004; 430:88–93. [PubMed: 15190252]
22. Dunker AK, Cortese MS, Romero P, Iakoucheva LM, Uversky VN. Flexible Nets. The Roles of Intrinsic Disorder in Protein Interaction Networks. FEBS J. 2005; 272:5129–5148. [PubMed: 16218947]

23. Haynes C, Oldfield CJ, Ji F, Klitgord N, Cusick ME, Radivojac P, Uversky VN, Vidal M, Iakoucheva LM. Intrinsic Disorder is a Common Feature of Hub Proteins from Four Eukaryotic Interactomes. PLoS Comput. Biol. 2006; 2:e100. [PubMed: 16884331]
24. Schatz PJ, Cull MG, Martin EL, Gates CM. Screening of Peptide Libraries Linked to Lac Repressor. Methods Enzymol. 1996; 267:171–191. [PubMed: 8743316]
25. Schuck P. Use of Surface Plasmon Resonance to Probe the Equilibrium and Dynamic Aspects of Interactions between Biological Macromolecules. Annu. Rev. Biophys. Biomol. Struct. 1997; 26:541–566. [PubMed: 9241429]
26. Delaglio F, Grzesiek S, Vuister GW, Zhu G, Pfeifer J, Bax A. NMRPipe: A Multidimensional Spectral Processing System Based on UNIX Pipes. J. Biomol. NMR. 1995; 6:277–293. [PubMed: 8520220]
27. Demeler, B. UltraScan: A Comprehensive Data Analysis Software Package for Analytical Ultracentrifugation Experiments. In: Scott, DJ.; Harding, SE.; Rowe, AJ., editors. Modern Analytical Ultracentrifugation: Techniques and Methods. Cambridge, U.K.: Royal Society of Chemistry; 2005. p. 210-229.
28. Laue, TM.; Shah, BD.; Ridgeway, TM.; Pelletier, SL. Computer-Aided Interpretation of Analytical Sedimentation Data for Proteins. In: Harding, SE.; Rowe, AJ.; Horton, JC., editors. Analytical Ultracentrifugation in Biochemistry and Polymer Science. Cambridge, U.K.: Royal Society of Chemistry; 1992. p. 90-125.
29. Durchschlag, H. Specific Volumes of Biological Macromolecules and some Other Molecules of Biological Interest. In: Hinz, H., editor. Thermodynamic Data for Biochemistry and Biotechnology. New York: Springer-Verlag; 1986. p. 45-128.
30. Gorfinkiel N, Fanti L, Melgar T, Garcia E, Pimpinelli S, Guerrero I, Vidal M. The *Drosophila* Polycomb Group Gene Sex Combs Extra Encodes the Ortholog of Mammalian Ring1 Proteins. Mech. Dev. 2004; 121:449–462. [PubMed: 15147763]
31. Czypionka A, de los Panos OR, Mateu MG, Barrera FN, Hurtado-Gomez E, Gomez J, Vidal M, Neira JL. The Isolated C-Terminal Domain of Ring1B is a Dimer made of Stable, Well-Structured Monomers. Biochemistry. 2007; 46:12764–12776. [PubMed: 17935356]
32. Satijn DP, Otte AP. RING1 Interacts with Multiple Polycomb-Group Proteins and Displays Tumorigenic Activity. Mol. Cell. Biol. 1999; 19:57–68. [PubMed: 9858531]
33. Garcia E, Marcos-Gutierrez C, del Mar Lorente M, Moreno JC, Vidal M. RYBP, a New Repressor Protein that Interacts with Components of the Mammalian Polycomb Complex, and with the Transcription Factor YY1. EMBO J. 1999; 18:3404–3418. [PubMed: 10369680]
34. Kaneko T, Miyagishima H, Hasegawa T, Mizutani-Koseki Y, Isono K, Koseki H. The Mouse YAF2 Gene Generates Two Distinct Transcripts and is Expressed in Pre-and Postimplantation Embryos. Gene. 2003; 315:183–192. [PubMed: 14557078]
35. Sakamoto Y, Watanabe S, Ichimura T, Kawasuji M, Koseki H, Baba H, Nakao M. Overlapping Roles of the Methylated DNA-Binding Protein MBD1 and Polycomb Group Proteins in Transcriptional Repression of HOXA Genes and Heterochromatin Foci Formation. J. Biol. Chem. 2007; 282:16391–16400. [PubMed: 17428788]
36. Sanchez C, Sanchez I, Demmers JA, Rodriguez P, Strouboulis J, Vidal M. Proteomics Analysis of Ring1B/Rnf2 Interactors Identifies a Novel Complex with the Fbxl10/Jhdm1B Histone Demethylase and the Bcl6 Interacting Corepressor. Mol. Cell. Proteomics. 2007; 6:820–834. [PubMed: 17296600]

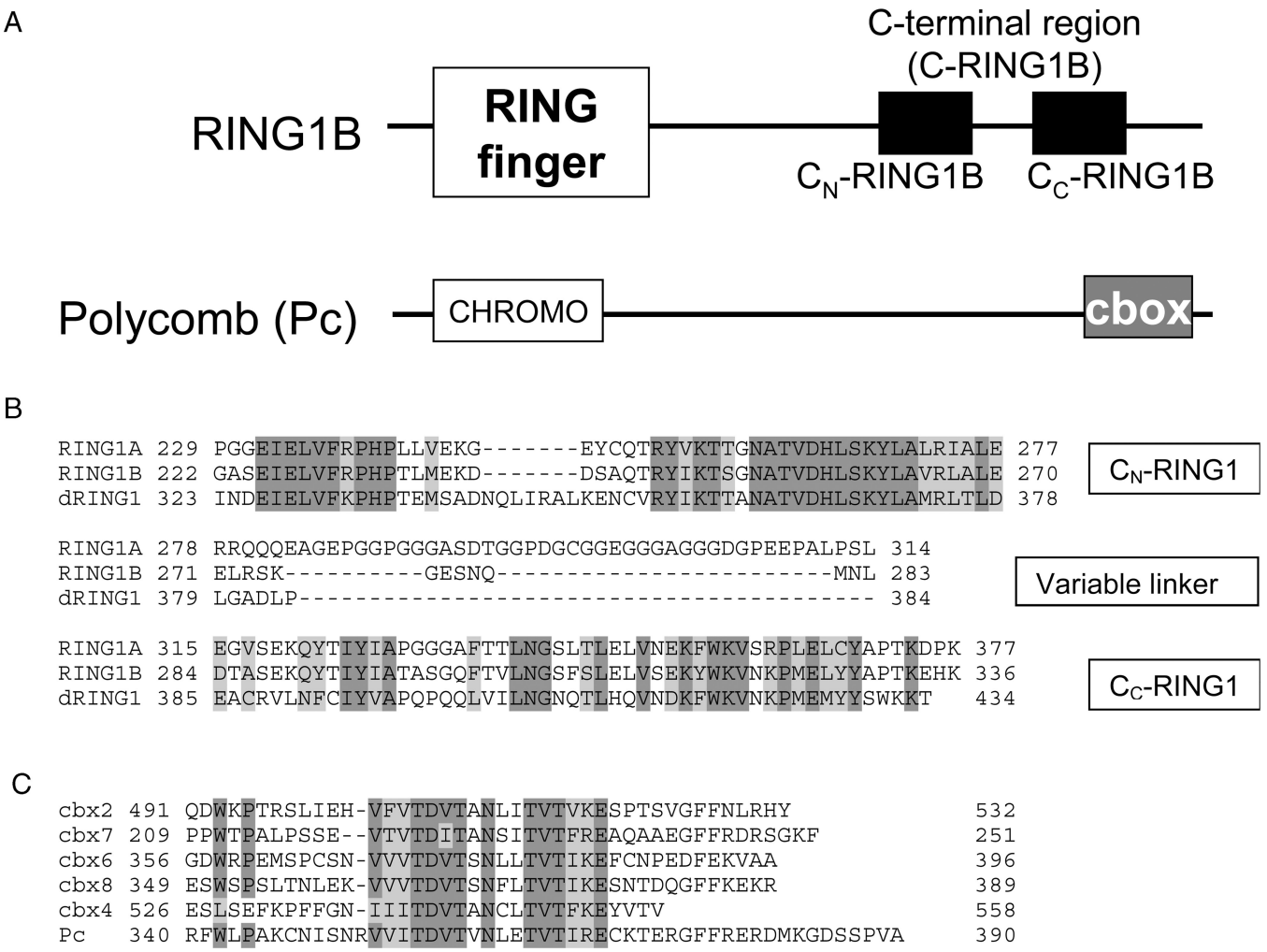

Figure 1.

RING1 and Pc proteins. (A) Domain structure of RING1B and the Pc proteins. (B) Sequence alignment of human RING1A and RING1B and *Drosophila* RING1 (dRING1). Identical residues in the alignment are highlighted in dark gray, and functionally similar residues are highlighted in light gray. The C-RING1 sequence alignment is divided into three segments: the N-terminal half (or C_NRING1), the variable linker, and the C-terminal half (C_C-RING1). (C) Sequence alignment of the human Pc cbox domains and the *Drosophila* Pc cbox domain (Pc). The residues shown here are the ones used in this study. The shading is the same as in panel B.

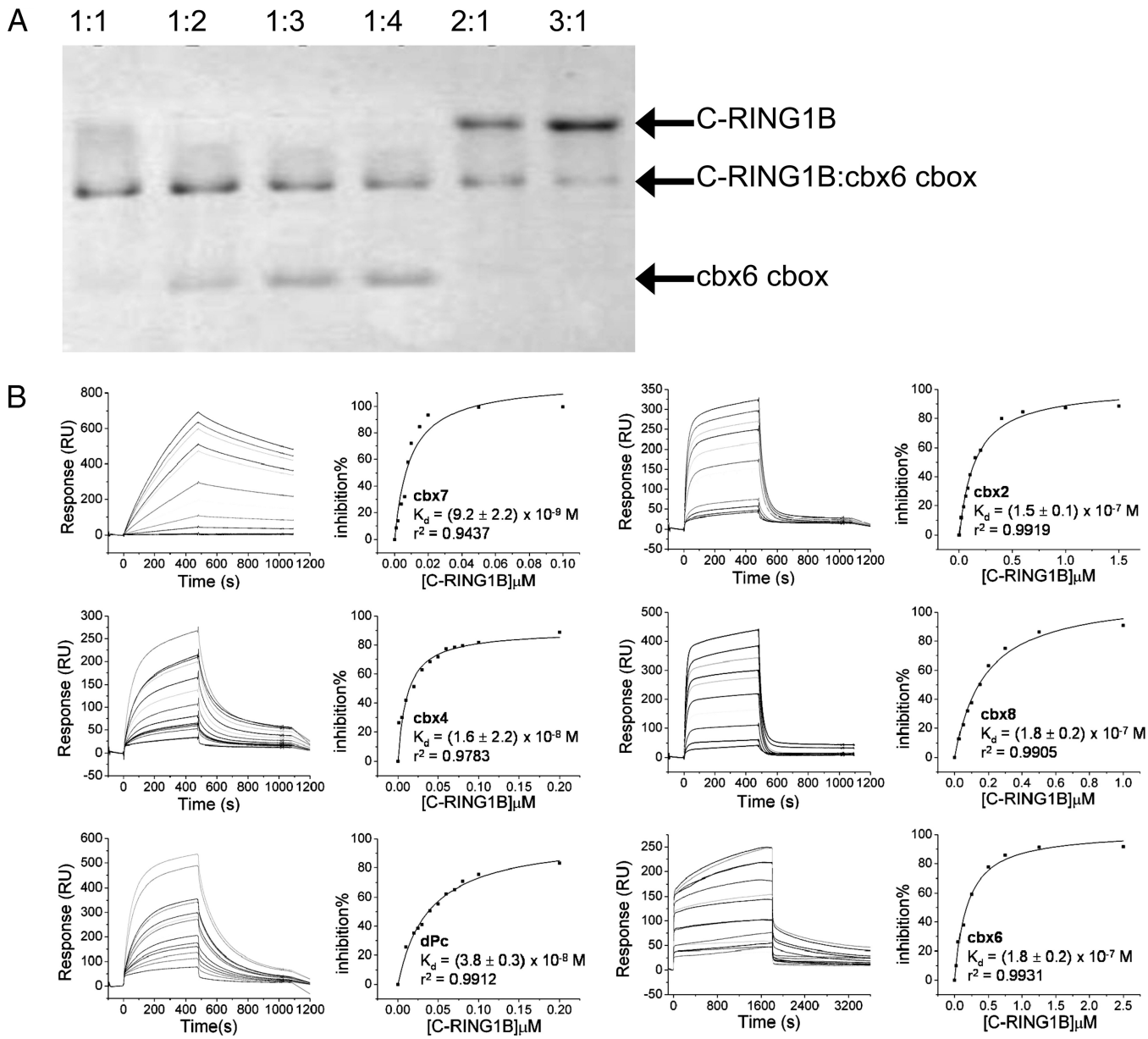

Figure 2.

Analysis of the C-RING1B–cbox domain interaction. (A) Native gel electrophoresis to determine the binding stoichiometry of C-RING1B to cbox. The gel lanes indicate the C-RING1B:cbx6 cbox molar ratios. The first four gel lanes use 0.68 nmol of C-RING1B, and the last two use 0.68 nmol of the cbx6 cbox domain. The gel bands are identified by the arrows. (B) Solution competition titrations of the MBP–cbox domain proteins binding to C-RING1B cross-linked onto the immobile phase competed away with varying amounts of C-RING1B in the mobile phase are shown for each of the Pc cbox proteins. The fits of the competition titration experiments to a hyperbolic function are shown to the right of the raw SPR data. The inset in the binding curve identifies the Pc orthologue. The standard error and r^2 values for the fit are also shown in the insets.

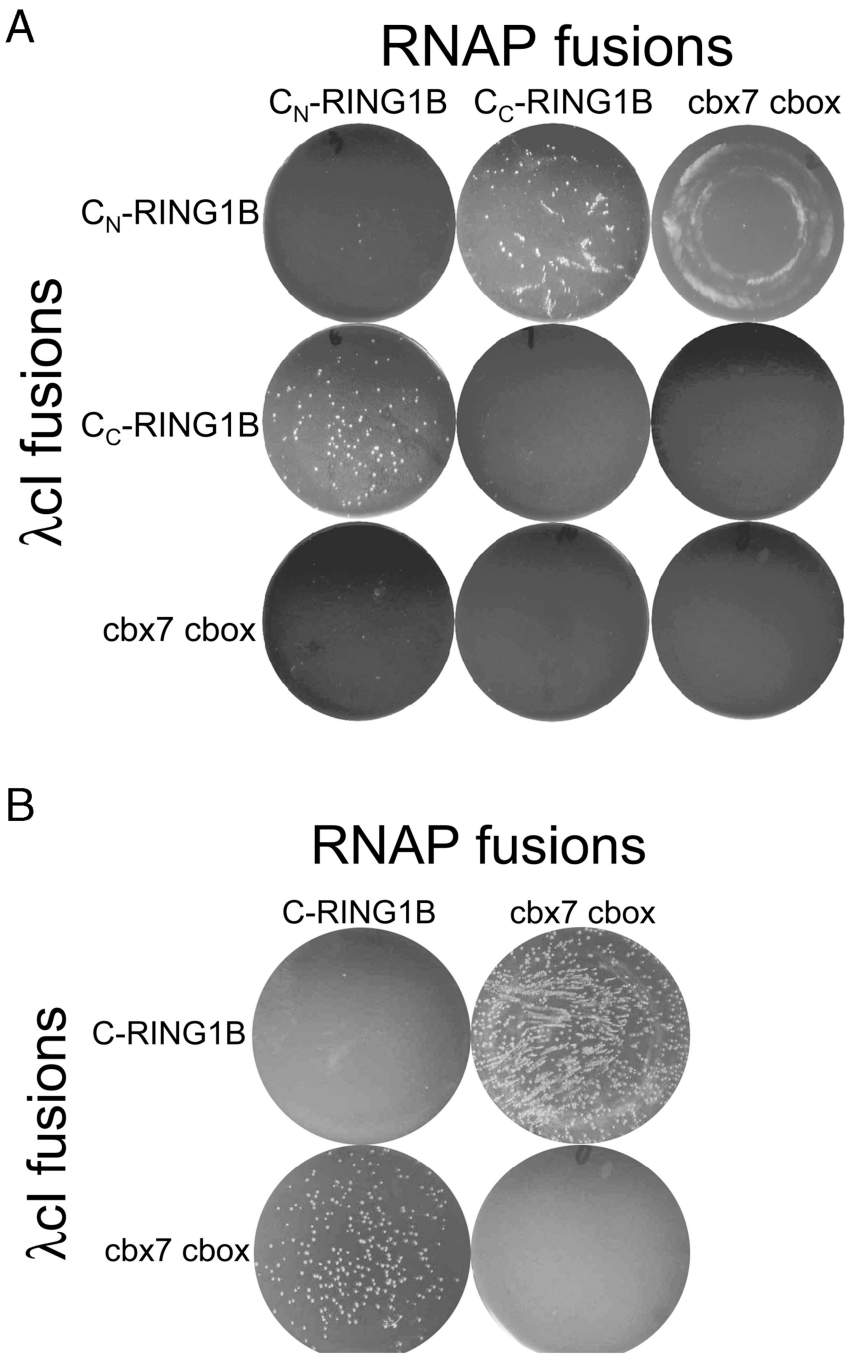

Figure 3.

C-RING1B is composed of two interacting subregions. (A) The bacterial two-hybrid assay utilizes the DNA binding properties of λ cI and the transcriptional activation properties of the N-terminal domain of RNA polymerase (RNAP). The two subregions of C-RING1B, C_N-RING1B and C_C-RING1B, are cloned as a fusion with either λ cI or RNAP and cotransformed into Bacteriomatch reporter cells (Strategene). Interaction between λ cI and RNAP fusion proteins results in the recruitment of RNAP to the promoter, activating transcription of the β-lactamase gene and conferring ampicillin resistance to the transformed

bacteria. (B) Positive control showing the interaction between the entire C-RING1B and the cbx7 cbox domain.

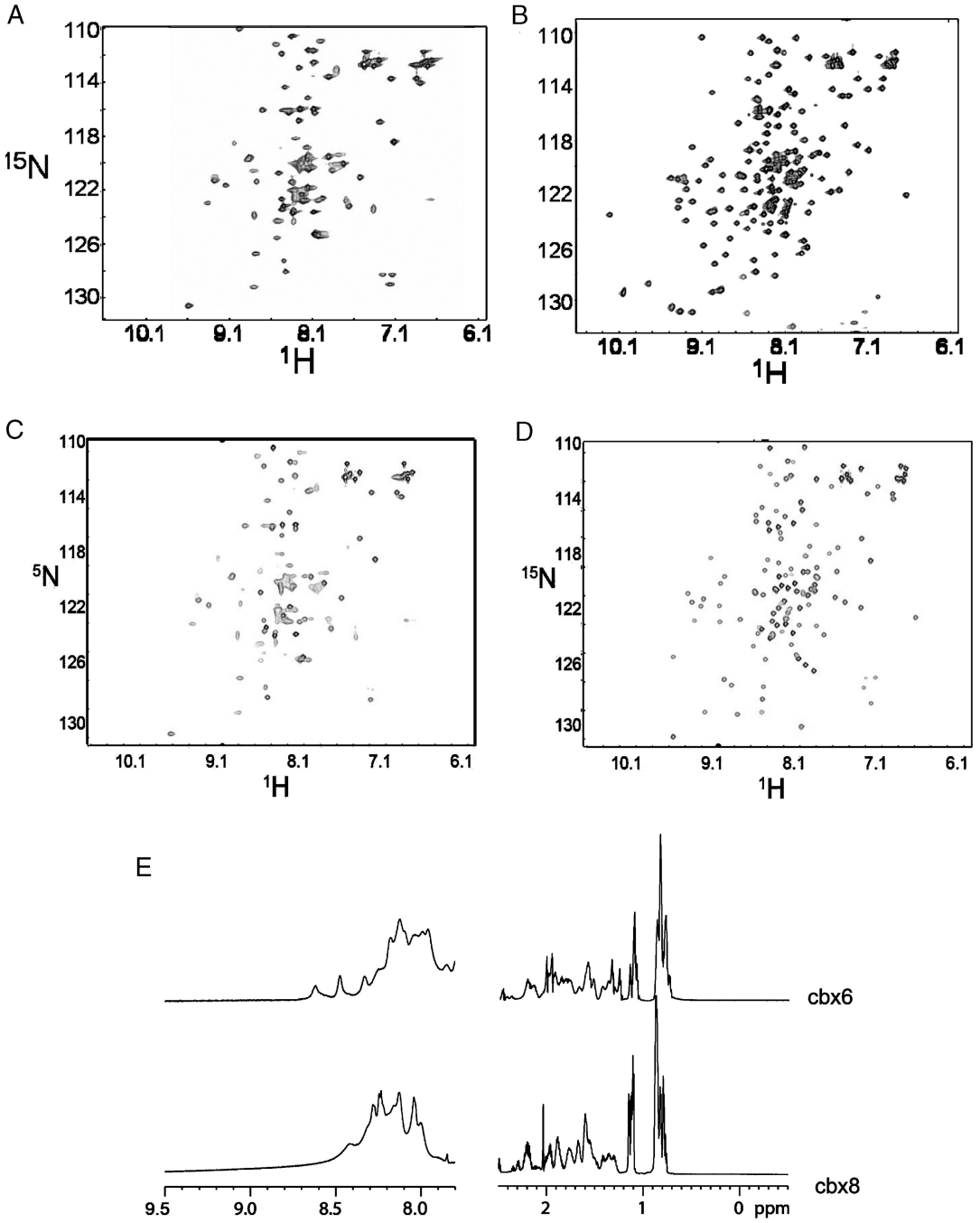

Figure 4.

NMR characterization of C-RING1B and the cbox domain. Two-dimensional $^{1}H–^{15}N$ HSQC spectroscopy of (A) C-RING1B alone and (B) the C-RING1B–cbx7 cbox domain complex. (C) Same as panel A but at 100 mM C-RING1B. (D) Same protein sample that was used for panel C but with unlabeled equimolar cbx8 cbox added. The lighter shaded chemical shifts are “folded” peaks corresponding to chemical shifts which occur beyond the indicated spectral width. (E) One-dimensional ^{1}H NMR spectra of the cbx6 and cbx8 cbox domains.

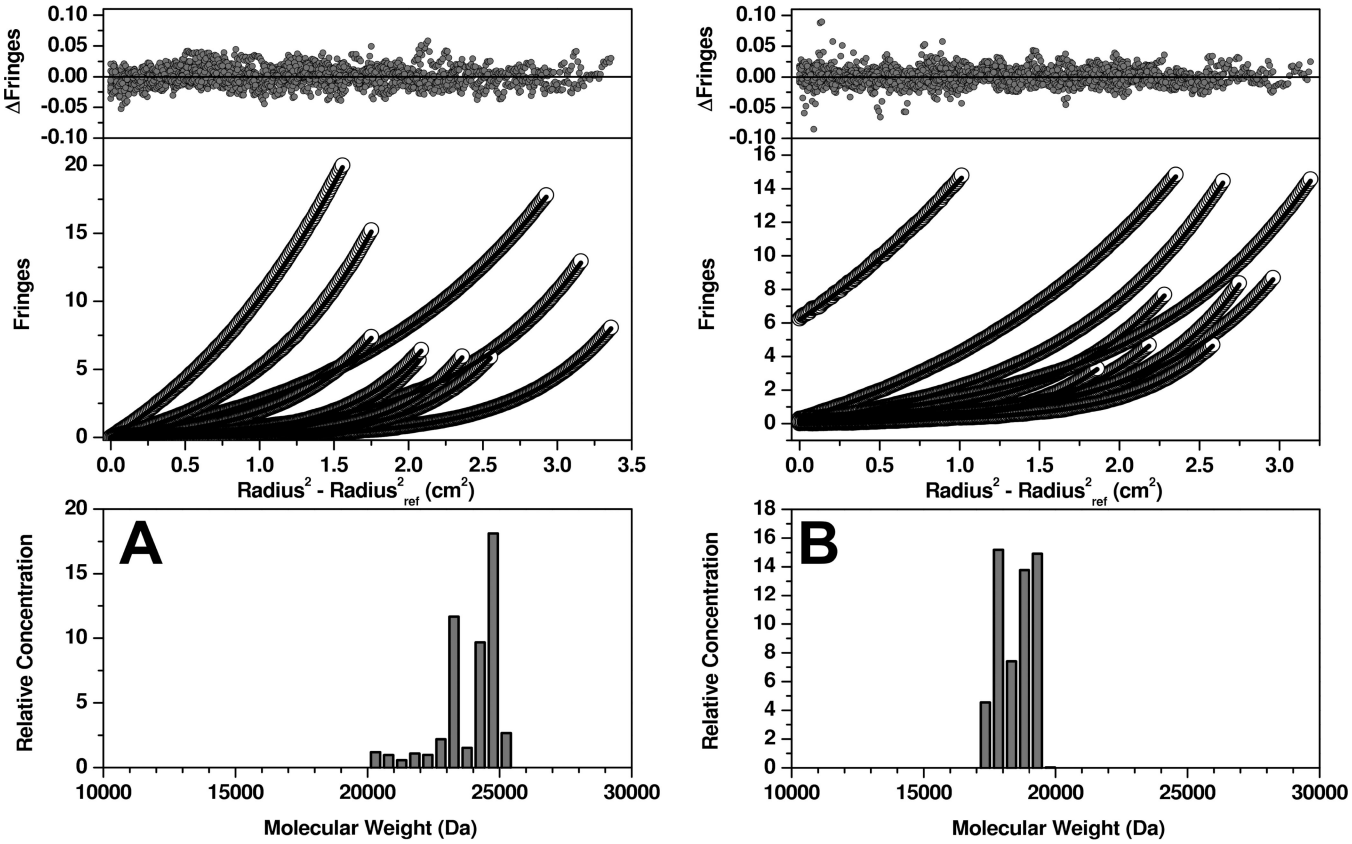

Figure 5.

Sedimentation equilibrium analysis of C-RING1B alone (A) and the C-RING1B–cbx7 cbox domain complex (B). Data from multiple rotor speeds and loading concentrations were fitted globally with UltraScan. In the top panel of both figures, the residuals of each fit are shown. In the center panels, the experimental data (○) and the fitted model (—) are shown as overlays. The bottom panels show the molecular mass distributions derived from the fits using a fixed molecular mass distribution model.